3D Fingerprint Phantoms

Sunpreet S. Arora, Kai Cao and Anil K. Jain
Department of Computer Science and Engineering
Michigan State University
East Lansing, Michigan 48824
Email: {arorasun, kaicao, jain}@cse.msu.edu

Nicholas G. Paulter Jr.
National Institute of Standards and Technology
100 Bureau Dr. Gaithersburg, Maryland 20899
Email: paulter@nist.gov

Abstract—One of the critical factors prior to deployment of any large scale biometric system is to have a realistic estimate of its matching performance. In practice, evaluations are conducted on the operational data to set an appropriate threshold on match scores before the actual deployment. These performance estimates, though, are restricted by the amount of available test data. To overcome this limitation, use of a large number of 2D synthetic fingerprints for evaluating fingerprint systems had been proposed. However, the utility of 2D synthetic fingerprints is limited in the context of testing end-to-end fingerprint systems which involve the entire matching process, from image acquisition to feature extraction and matching. For a comprehensive evaluation of fingerprint systems, we propose creating 3D fingerprint phantoms (phantoms or imaging phantoms are specially designed objects with known properties scanned or imaged to evaluate, analyze, and tune the performance of various imaging devices) with known characteristics (e.g., type, singular points and minutiae) by (i) projecting 2D synthetic fingerprints with known characteristics onto a generic 3D finger surface and (ii) printing the 3D fingerprint phantoms using a commodity 3D printer. Preliminary experimental results show that the captured images of the 3D fingerprint phantom can be successfully matched to the 2D synthetic fingerprint images (from which the phantom was generated) using a commercial fingerprint matcher. This demonstrates that our method preserves the ridges and valleys during the 3D fingerprint phantom creation process ensuring that the synthesized 3D phantoms can be utilized for comprehensive evaluations of fingerprint systems.

I. INTRODUCTION

Faulds, Galton and Henry were the pioneers in formalizing the scientific basis of using fingerprints for person identification in the late 19th century [1]. Until about 20 years ago, fingerprints were primarily used by law enforcement agencies to identify criminals. However, of late, fingerprints are being extensively used in civilian and commercial applications. Examples of some of the large scale operational fingerprint recognition systems include (i) "Aadhar" to assign a unique identification number to each resident of India [2], (ii) the system to prevent criminals and immigration violators from crossing the United States border by the Office of Biometric Identity Management Identification Services (formerly the US-VISIT program) [3], (iii) the finger scan system deployed at Walt Disney World Theme Parks to help prevent the use of stolen or fraudulent tickets for entering their premises [4], and (iv) the TouchID system in the Apple iPhone 5s for authenticating mobile phone users [5].

Before the deployment of any large scale biometric system, one of the critical factors is to have a reasonable estimate of the matching performance of the system in the operational set-
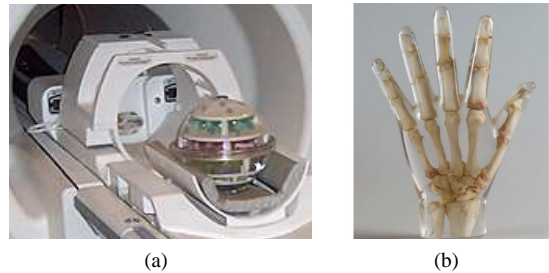

Fig. 1. Examples of imaging phantoms used in medical imaging: (a) Phannie, a phantom to calibrate MRI machines developed at NIST [7], and (b) a phantom hand used for evaluating X-ray machines [8].

tings. For this purpose, typically, several pilot studies are first conducted in the field to ascertain the operational thresholds to achieve the desired False Accept Rate (FAR). This is a tedious process both in terms of time and resources. Besides, the resulting performance estimate is limited by the amount and nature of data which is available. One of the possible solutions to alleviate this shortcoming is to synthetically generate very large amounts of realistic biometric data which can then be used for system performance evaluation. In case of fingerprint systems, this would entail generating, say millions of synthetic fingerprints for evaluating fingerprint recognition systems [6].

State of the art 2D synthetic fingerprint generators [9], [10] output 2D synthetic fingerprints using mathematical or statistical models of fingerprint features (e.g. fingerprint type, orientation field and minutiae). The 2D synthetic fingerprint generator proposed in [9] generates ridge flow map using a mathematical model and ridge density map based on heuristics learned from several fingerprint images. Directional filters tuned to local ridge orientation and frequency values are then iteratively applied starting from a few seed locations to generate fingerprint ridge patterns. Note, however, that minutiae placement cannot be controlled during the 2D synthetic fingerprint generation process. On the other hand, the 2D synthetic fingerprint generation method in [10] outputs 2D synthetic fingerprints using statistical models of fingerprint features (fingerprint type, orientation field and minutiae). The features are first sampled from their respective statistical distributions, followed by a fingerprint reconstruction method (described in [11]) to generate visually realistic synthetic fingerprints.

While these methods can be used to generate synthetic fingerprints to evaluate fingerprint feature extraction and matching algorithms, their usage is limited in the context of evaluating an end-to-end fingerprint biometric system, from

Method	Artifacts	Fingerprint Features	Evaluation Use Cases
SFinGe [9]	2D synthetic fingerprints (electronic)	Known fingerprint ridge flow and ridge density features; uncontrolled minutiae placement	Fingerprint feature extractors and matchers
Zhao et al. [10]	2D synthetic fingerprints (electronic)	Known fingerprint ridge flow, ridge density and minutiae features	Fingerprint feature extractors and matchers
Proposed	3D fingerprint phantoms (electronic and physical)	Known fingerprint ridge flow, ridge density and minutiae features	End-to-end fingerprint systems, including fingerprint sensors, feature extractors and matchers

sensing a finger and acquiring its impression to extracting the template and establishing or verifying an identity (Table I). For example, the 2D synthetic fingerprint generators are inadequate for testing touchless fingerprint sensing technologies [12], [13] which have been gaining prominence as alternatives to the traditional touch based fingerprint capture systems. This is primarily because these approaches, e.g., [9] and [10], only generate synthetic fingerprints as 2D electronic artifacts or images.

In this research, we propose to generate synthetic fingerprints as 3D artifacts (both as 3D electronic artifacts and 3D physical artifacts) which could be used for an exhaustive evaluation of fingerprint systems. These 3D artifacts can be made to have prespecified physical dimensions of the human fingers and properties of the finger material (e.g. hardness, electrical conductivity) as well as fingerprint type (e.g., arch, loop and whorl), singular points and minutiae positions. In this way, the 3D fingerprint phantoms differ from "silicone" and "gummy" fingers [14] [15] aimed specifically at vulnerability analysis of fingerprint recognition systems where fingerprint features are not known apriori. Our objective in generating 3D fingerprint artifacts is quite similar, in essence, to *imaging phantoms* (see Fig. 1) which are specially designed objects with known properties used for calibrating and testing optical measurement profiles of sensing instrumentation in the biomedical domain [16], [17]. We coin the term *3D fingerprint phantoms* for the 3D synthetic artifacts created for the purpose of evaluating end-to-end fingerprint recognition systems.

The 3D fingerprint phantoms are created using a state of the art 2D synthetic fingerprint generation method [10] and a generic 3D model of the finger surface[1]. The 3D finger surface is first aligned such that the finger length is along the y-axis, width along the x-axis and depth along the z-axis. This is followed by mapping the 2D fingerprint image onto the 3D finger surface for establishing correspondences between each vertex on the 3D surface and the 2D fingerprint image texture. Finally, the fingerprint ridges and valleys are engraved onto the 3D finger surface by displacing each vertex along the surface normal according to the mapped texture values. The 3D fingerprint phantoms are printed using a commodity 3D printer and then imaged using two different state of the art smartphone cameras. Preliminary experimental results show that the captured images of the 3D fingerprint phantoms can be successfully matched to the 2D synthetic fingerprint images used to generate the fingerprint phantoms using a state of the art commercial fingerprint matcher. This demonstrates that the

ridges and valleys in the 2D synthetic fingerprint image are preserved when mapping it to the 3D surface of the fingerprint phantom. Thus, the 3D fingerprint phantoms created in this way can be utilized for comprehensive evaluation of fingerprint systems.

II.   SYNTHESIZING 3D FINGERPRINT PHANTOM

A 3D fingerprint phantom P is synthesized from a 2D synthetic fingerprint image I with known fingerprint features generated using a state of the art 2D synthetic fingerprint generator, and a generic 3D finger surface S. Let the texture values in the 2D fingerprint image I at spatial coordinates (u, v) be denoted by $I(u, v)$. Also, assume that the 3D finger surface S is a triangular mesh having a set of vertices V and triangles T. Each vertex in V has (x, y, z) coordinates corresponding to its spatial location; a triangle in T connects a unique set of three vertices. Synthesizing a 3D fingerprint phantom P using I and S then consists of the following steps:

1) *Surface Preprocessing*: Preprocess the 3D finger surface S to remove outlier vertices and triangles and make the surface sufficiently dense for engraving ridges and valleys.
2) *Surface Alignment*: Align the 3D finger surface S such that the finger length is along the y-axis.
3) *Surface Parametrization*: Determine the mapping between the (x, y, z) spatial locations of the vertices on the 3D surface S and the (u, v) image domain of the 2D synthetic fingerprint image I to obtain the parameterized 3D finger surface S_P.
4) *Vertex Displacement*: Displace the vertices in S along the surface normals according to the texture values in the 2D synthetic fingerprint I at the mapped (u, v) locations to engrave ridges and valleys on the parameterized finger surface S_P.
5) *Surface Postprocessing and 3D Phantom Printing*: Synthetically create a cuboidal support beneath the 3D surface S_P and prespecify the physical dimensions as well as the printing material according to the physical properties of the finger such as hardness and electrical conductivity before printing the 3D fingerprint phantom P using a commodity 3D printer.

A detailed description of each of these steps used in the 3D fingerprint phantom creation process for a given 2D synthetic fingerprint image I and a 3D finger surface S is given below.

A. Surface Preprocessing

The generic finger surface S is first preprocessed to remove the vertices and triangles which lie far away from the main part

---

[1]The 3D finger surface could be either the shape of the finger sensed using a 3D fingerprint scanner or a synthetically generated surface describing the shape of the finger. In our case, the finger surface was obtained using a 3D fingerprint scanner.
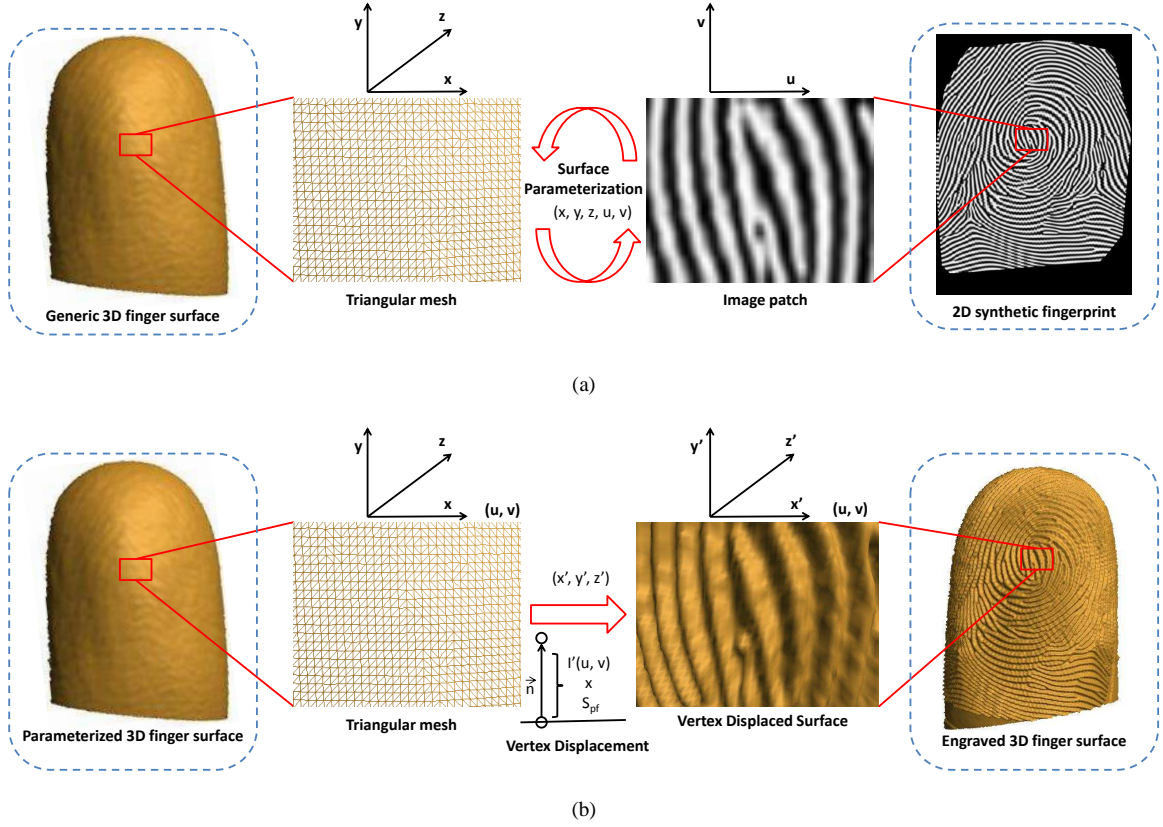
Fig. 2. Illustrating the two major steps of (a) surface parameterization, and (b) vertex displacement in synthesizing a 3D fingerprint phantom from a 2D synthetic fingerprint image and a generic 3D finger surface.

of the finger surface. This is done by clustering the vertices in V according to a distance threshold d on the length of edges in each triangle in T. In other words, if the length of the edge connecting two vertices in a triangle is smaller than d, they belong to the same cluster; otherwise they are grouped in a different cluster. The largest cluster of vertices V_R and triangles T_R obtained as a result of this clustering process is then retained in the finger surface S, whereas the vertices and triangles pertaining to other smaller clusters are discarded.

The finger surface S also needs to be made sufficiently dense for engraving ridges and valleys. This is done by sampling points at the centroid of each retained triangle in T_R and connecting each of the three vertices to the centroid of the triangle. Let the set of vertices and triangles obtained after this process be denoted by V_D and T_D, respectively[2].

B. Surface Alignment

Each vertex in V_D is translated such that the center of the surface S coincides with the origin of the (x, y, z) coordinate axes. Principal component analysis (PCA) [18] is used to determine the principle directions of the surface spread. The computed principal components are used to align the surface S such that the finger length is along the y-axis, width along the x-axis and height on the z-axis. Note that this method only affects the (x, y, z) coordinate values of the vertices in V_D.

[2]The generic 3D finger surface used in our experiments has 58,494 vertices and 115,975 triangles and is already sufficiently dense; $V_D = V_R$ and $T_D = T_R$ in our case.

C. Surface Parameterization

This step involves projecting the 2D synthetic fingerprint image I onto the 3D finger surface S. For this mapping, the one-to-one correspondence between the image coordinates (u, v) in I and the spatial locations (x, y, z) in S needs to be established. This process, in general, is termed *surface parameterization* and is used extensively for geometric modelling of 3D objects [19]. We adopt the surface parameterization method proposed in [20] for determining the injective mapping from the (u, v) image domain to the finger surface S.

Recall that the aligned finger surface S is in the form of a triangular mesh i.e. the union of a set of triangles $T_D = \{T_D^1, ..., T_D^N\}$, where N is the number of triangles. The goal of discrete harmonic mapping is to find the planar (u, v) domain representation $S^* \subset R^2$ of S using a piecewise linear map $f : S \to S^*$ which minimizes the Dirichlet energy E_D, where

$$E_D = \frac{1}{2} \int_S ||\nabla_S f||^2 = \frac{1}{2} \sum_{i=1}^{N} \int_{T_D^i} ||\nabla_{T_D^i} f||^2. \quad (1)$$

Here ∇_S denotes the gradient over the finger surface S, and $\nabla_{T_D^i}$ is the gradient over the surface formed by each triangle T_D^i in S. Note that the minimization procedure is subject to natural boundary condition [20].

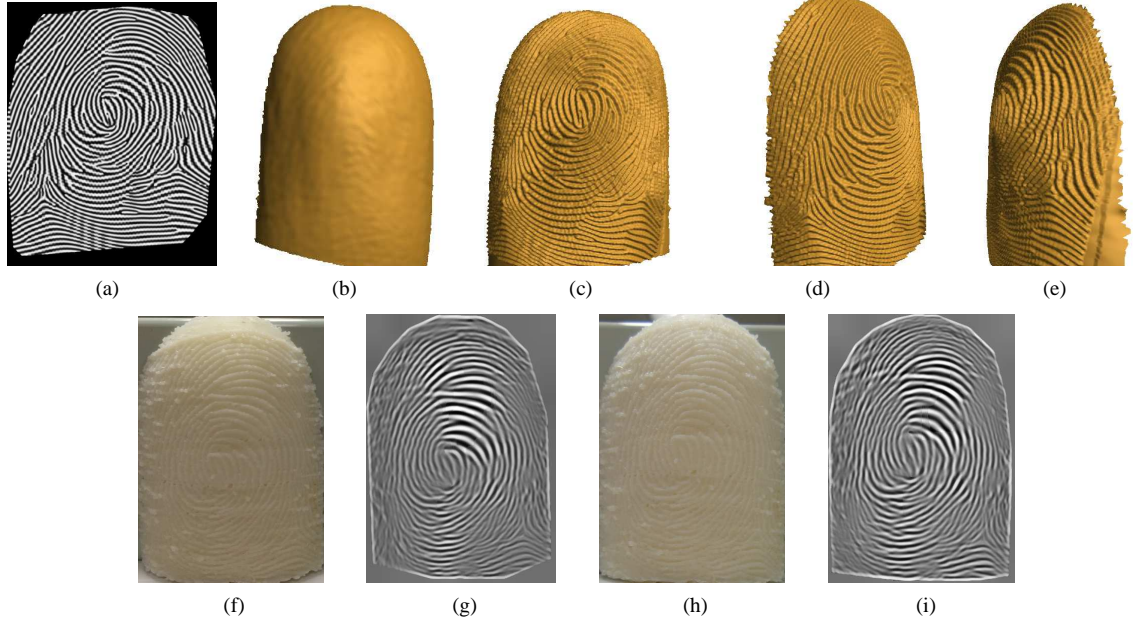Let p_j denote the jth vertex of the triangle T_D^i such that

Fig. 3. 2D synthetic image to 3D fingerprint phantom. (a) A sample 2D synthetic fingerprint image generated using the method in [10]; (b) generic 3D finger surface; (c) the frontal view, (d) the left profile view and (e) the right profile view of the electronic 3D fingerprint phantom created by mapping (a) onto (b); (f) and (h) the 2D images of the printed 3D fingerprint phantom captured using the 8MP and 16 MP smartphone cameras, respectively; (g) and (i) the enhanced 2D images of (f) and (h).

$1 \leq j \leq 3$. Also let θ_j be the angle opposite to vertex p_j in T_D^i. Then, it can be shown that

$$2 \int_{T_D^i} ||\nabla_{T_D^i} f||^2 = \cot \theta_3 ||f(p_1) - f(p_2)||^2$$
$$+ \cot \theta_2 ||f(p_3) - f(p_1)||^2 + \cot \theta_1 ||f(p_3) - f(p_2)||^2 \quad (2)$$

Under the piecewise linear assumption in Eq. (1), the minimization problem for the kth vertex p_k in the set V_D reduces to solving a system of linear equations pertaining to the set of triangles τ which share the common vertex p_k

$$\sum_{\triangle_{p_k, p_l, p_m} \in \tau} \cot \alpha (f(p_k) - f(p_l)) + \cot \beta (f(p_k) - f(p_m))$$
$$= \sum_{\triangle_{p_k, p_l, p_m} \in \tau} R^{90} (f(p_m) - f(p_l)). \quad (3)$$

Here α and β are the angles at the other two vertices p_l and p_m in a triangle with vertices p_k, p_l and p_m in τ, and R^{90} denotes a $90°$ rotation.

The mapping between the 3D finger surface in (x, y, z) and the (u, v) image domain obtained by solving the system of linear equations in Eq. (3) may be globally inconsistent with respect to translation, rotation and scale. To ensure global consistency of correspondences, we enforce translation, rotation and scale constraints:

- The translation constraint ensures the origin in S^* is at a fixed distance d' below the reference point detected on the fingerprint image I using the method described in [21]. This distance d' is set to 50 pixels in our experiments.

- The rotation constraint ensures that the y-axis in S^* coincides with the v-axis of the (u, v) domain.

- The scale constraint ensures that the mapped (u, v) texture from the 2D synthetic fingerprint image I occupies the maximum surface area on the 3D surface S.

In summary, the 3D finger surface S is parameterized using the piecewise linear mapping $f : S \rightarrow S^*$, where $S^* \subset R^2$ such that each vertex p of the parameterized surface S_P is denoted as a 5-tuple (x, y, z, u, v) pertaining to its spatial location (x, y, z) on the surface and the (u, v) locations of the texture values from the 2D synthetic fingerprint image I (Fig. 2 (a)).

D. Vertex Displacement

In the penultimate step, vertices are displaced along their surface normals to engrave the fingerprint ridges and valleys on S_P (Fig. 2 (b)). Let the normal at a vertex $p(x, y, z, u, v)$ be denoted by (n_x, n_y, n_z), where n_x, n_y and n_z represent the normal components along the x, y and z directions, respectively. The displaced coordinates of the vertex (x', y', z') along the normal are then computed using the principle of vertex displacement mapping [22] as follows:

$$\begin{bmatrix} x' \\ y' \\ z' \end{bmatrix} = \begin{bmatrix} x \\ y \\ z \end{bmatrix} - \begin{bmatrix} n_x \\ n_y \\ n_z \end{bmatrix} \times I'(u, v) \times S_{pf} \quad (4)$$

Here, $I'(u,v)$ is the scale normalized texture value in the range $[-1,1]$ of the mapped (u,v) texture from the 2D synthetic fingerprint image on the vertex (x,y,z), and S_{pf} the surface perturbation factor which depends on the scale of the generic 3D finger surface. It is set to 2.5×10^{-6} for the finger surface used in our experiments.

E. Surface Postprocessing and 3D Phantom printing

The vertex displaced 3D finger surface S_P is printed using a commodity 3D printer to create the 3D fingerprint phantom P. To ensure stability of the finger surface S_P, a cuboidal support is synthetically created beneath the surface before printing. The physical dimensions of the fingerprint phantom P and the printing material are explicitly specified according to the desired finger characteristics such as hardness and electrical conductivity.

III. EVALUATION

For our preliminary experimental evaluation, four 3D fingerprint phantoms were printed at the preset highest resolution setting using a commodity 3D printer with hard plastic ABS 1.8 mm filament as the printing material[3]. The physical length of the phantoms was fixed to be 6 cm (including the cuboidal support of around 1 cm) with the aspect ratio of the other two dimensions maintained during scaling. Frontal images of these phantoms were then captured using two state of the art smartphone cameras[4], an 8 MP camera and a 16 MP camera. Images were acquired with a standoff of 10 cm with the cameras in their default settings.

A. Matching Performance

To gauge the effectiveness of the 3D fingerprint phantom, two different matching experiments were performed. 3D fingerprint phantoms created using (i) original 2D finger impressions, and (ii) 2D synthetic fingerprint images.

1) Experiment I: In Experiment I, 3D fingerprint phantoms were created using two search impressions, S0005 and S0010, from the NIST Special Database 4 [23]. Region of Interest (ROI) and ridge orientation field of the fingerprint images were estimated using the NIST Biometric Image Software [24] and ridge frequency was computed using the method described in [25]. The impressions were enhanced using the estimated ridge orientation and ridge frequency field and demodulated using the method in [26] to ensure sufficient contrast between ridges and valleys before projecting them onto the 3D finger surface. The 2D images of 3D fingerprint phantoms captured using the two smartphone cameras were enhanced using manually marked ridge orientation and ridge frequency field. They were then scaled down based on the ridge frequency difference between the images and their original impressions and matched to their original impressions S0005 and S0010 as well as their respective file impressions F0005 and F0010 in NIST SD4 using a commercial fingerprint matcher (see Fig. 4).

---

[3]While we would have liked to use soft materials for printing 3D fingerprint phantoms, the best available 3D printer we had access to only supported printing using hard filaments.

[4]Traditional contact based fingerprint capture systems could not be used for evaluation because the 3D fingerprint phantoms were printed using hard plastic.

TABLE II. EXPERIMENT I MATCH SCORES
(MATCH SCORE THRESHOLD IS 33 FOR VERIFICATION @ 0.01 % FAR)

	S0005	F0005		S0010	F0010
S0005_img1	134	77	S0010_img1	59	53
S0005_img2	101	77	S0010_img2	57	29

TABLE III. EXPERIMENT II MATCH SCORES
(MATCH SCORE THRESHOLD IS 33 FOR VERIFICATION @ 0.01 % FAR)

	Syn1		Syn2
Syn1_img1	101	Syn2_img1	90
Syn1_img2	107	Syn2_img2	92

Table II shows the match scores between the enhanced 2D images of 3D fingerprint phantoms captured using the 8 MP smartphone camera (S0005_img1 and S0010_img1) and the 16 MP smartphone camera (S0005_img2 and S0010_img2) to their original impressions (S0005 and S0010) and file impressions (F0005 and F0010), respectively. All, except one, match scores are higher than the computed threshold of 33 at 0.01% FAR for verification experiments on NIST SD4. In the identification experiments conducted using 2,000 file impressions in NIST SD4 as the gallery, both file impressions F0005 and F0010 are retrieved at rank-1. Thus, based on these preliminary experiments, we can conclude that features are preserved while mapping the 2D fingerprint image to the 3D finger surface.

2) Experiment II: In Experiment II, two 2D synthetic fingerprints Syn1 and Syn2, generated by a state of the art synthetic fingerprint generator [10], were used to create 3D fingerprint phantoms (see Figs. 3 (a)-(d)). Analogous to Experiment I, the 2D images of the 3D fingerprint phantoms were enhanced using manually marked ridge orientation and ridge frequency, and rescaled (see Figs. 3 (f)-(i)). These 2D images were then matched to the synthetic fingerprints from which they were created using a commercial fingerprint matcher.

Table III shows the match scores between the enhanced 2D images of 3D fingerprint phantoms captured using the 8 MP smartphone camera (Syn1_img1 and Syn2_img1) and the 16 MP smartphone camera (Syn1_img2 and Syn2_img2) to their original impressions Syn1 and Syn2, respectively. All match scores are above the threshold match score of 33 at a FAR of 0.01% computed for the verification experiments on NIST SD4. The original 2D synthetic fingerprints were matched at rank-1 in the identification experiments conducted using the 2,000 file fingerprints in NIST SD4 as the gallery. This shows that ridges and valleys are preserved during the 3D fingerprint phantom creation process.

IV. CONCLUSIONS AND FUTURE WORK

Evaluation of a biometric system is typically done by conducting several pilot studies in the field before its real world deployment. However, the performance estimate of the system is limited by the amount and nature of the available data. One possible solution is to synthetically generate data with known characteristics for evaluation purposes. In the context of evaluating end-to-end fingerprint recognition systems involving fingerprint image acquisition, feature extraction and matching, we present a procedure for creating 3D fingerprint phantoms by projecting 2D synthetic fingerprint images with
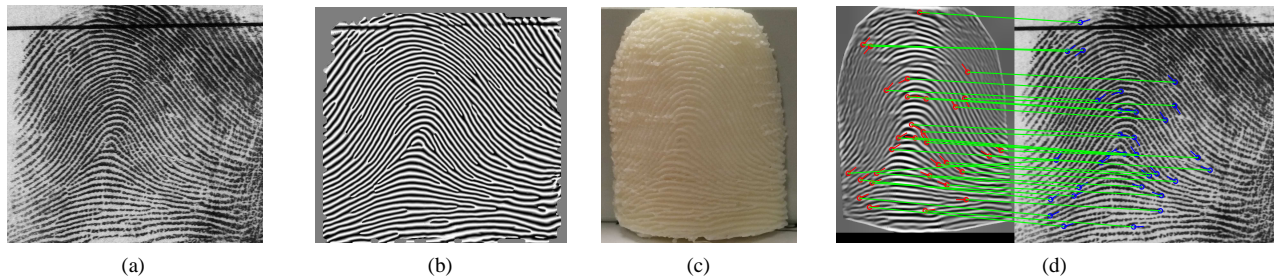
(a)   (b)   (c)   (d)

Fig. 4. Matching experiments. (a) 2D search impression S0005 in NIST SD4; (b) enhanced 2D image of (a) used for projection onto the 3D finger surface; (c) 2D image of the printed 3D fingerprint phantom captured using the 8 MP smartphone camera; (d) minutiae correspondences output by the commercial fingerprint matcher between the enhanced 2D image of the 3D fingerprint phantom shown in (c) to image in (a).

known fingerprint features onto a generic 3D finger surface. Preliminary experimental results demonstrate that fingerprint features of the 2D synthetic fingerprint images are preserved during this process. The fabricated 3D fingerprint phantoms can be used for comprehensive evaluation of fingerprint recognition systems.

The current surface parameterization method preserves the projection angles while mapping the 2D synthetic fingerprint image onto the 3D finger surface. This results in significant variations in ridge frequencies from the central part to the periphery of the 3D finger surface. In future, we will explore methods to preserve geodesic distances on the 3D finger surface so as to better preserve ridge frequency values when determining the mapping between the 2D synthetic fingerprint image and the 3D finger surface. In the next phase of this research, we will collaborate with the Materials Measurement Science Division at NIST to study physical properties of the human finger such as hardness and electrical conductivity. This would help us in making an informed choice of printing material for 3D fingerprint phantoms.

REFERENCES

[1] A. K. Jain, J. Feng, and K. Nandakumar, "Fingerprint matching," *Computer*, vol. 43, no. 2, pp. 36–44, 2010.

[2] "Unique Identification Authority of India," http://uidai.gov.in/.

[3] "Office of Biometric Identity Management Identification Services," http://www.dhs.gov/obim-biometric-identification-services.

[4] "Walt Disney World," https://disneyworld.disney.go.com/.

[5] "TouchID System," http://support.apple.com/kb/ht5949.

[6] R. Cappelli, D. Maio, and D. Maltoni, "Synthetic fingerprint-database generation," in *16th IEEE International Conference on Pattern Recognition*, vol. 3, 2002, pp. 744–747.

[7] "Meet Phannie, NIST's Standard "Phantom" for Calibrating MRI Machines," http://www.nist.gov/pml/electromagnetics/phannie_051110.cfm.

[8] "X-Ray Phantom Hand," http://www.anatomicalmodel.eu/x-ray-phantom-hand-transparent.

[9] R. Cappelli, "Sfinge: an approach to synthetic fingerprint generation," in *International Workshop on Biometric Technologies (BT2004)*, 2004, pp. 147–154.

[10] Q. Zhao, A. Jain, N. Paulter, and M. Taylor, "Fingerprint image synthesis based on statistical feature models," in *IEEE Fifth International Conference on Biometrics: Theory, Applications and Systems (BTAS)*, 2012, pp. 23–30.

[11] J. Feng and A. K. Jain, "Fingerprint reconstruction: from minutiae to phase," *IEEE Transactions on Pattern Analysis and Machine Intelligence*, vol. 33, no. 2, pp. 209–223, 2011.

[12] Y. Chen, G. Parziale, E. Diaz-Santana, and A. Jain, "3D touchless fingerprints: Compatibility with legacy rolled images," in *Biometrics Symposium: Special Session on Research at the Biometric Consortium Conference*, 2006, pp. 1–6.

[13] G. Parziale and Y. Chen, "Advanced technologies for touchless fingerprint recognition," in *Handbook of Remote Biometrics*, ser. Advances in Pattern Recognition, M. Tistarelli, S. Li, and R. Chellappa, Eds. Springer London, 2009, pp. 83–109.

[14] T. Matsumoto, H. Matsumoto, K. Yamada, and S. Hoshino, "Impact of artificial gummy fingers on fingerprint systems," in *Electronic Imaging*. International Society for Optics and Photonics, 2002, pp. 275–289.

[15] T. Matsumoto, "Gummy and conductive silicone rubber fingers importance of vulnerability analysis," in *Advances in Cryptology-ASIACRYPT 2002*. Springer, 2002, pp. 574–575.

[16] V. V. Tuchin, A. N. Bashkatov, E. A. Genina, V. I. Kochubey, V. V. Lychagov, S. A. Portnov, N. A. Trunina, D. R. Miller, S. Cho, H. Oh, B. Shim, M. Kim, J. Oh, H. Eum, Y. Ku, D. Kim, and Y. Yang, "Finger tissue model and blood perfused skin tissue phantom," pp. 78 980Z–78 980Z–11, 2011. [Online]. Available: http://dx.doi.org/10.1117/12.881604

[17] D. A. Boas, C. Pitris, and N. Ramanujam, *Handbook of Biomedical Optics*. Taylor & Francis, 2011.

[18] I. Jolliffe, *Principal Component Analysis*. Wiley Online Library, 2005.

[19] M. S. Floater and K. Hormann, "Surface parameterization: a tutorial and survey," in *Advances in Multiresolution for Geometric Modelling*, ser. Mathematics and Visualization. Springer, 2005, pp. 157–186.

[20] M. Desbrun, M. Meyer, and P. Alliez, "Intrinsic parameterizations of surface meshes," *Computer Graphics Forum*, vol. 21, no. 2, pp. 209–218, 2002.

[21] S. Yoon, K. Cao, E. Liu, and A. K. Jain, "LFIQ: Latent Fingerprint Image Quality," in *IEEE Sixth International Conference on Biometrics: Theory, Applications and Systems (BTAS)*, 2013 (To Appear).

[22] "Vertex Displacement Mapping using GLSL," http://www.ozone3d.net/tutorials/vertex_displacement_mapping_p02.php.

[23] "NIST Special Database 4," http://www.nist.gov/srd/nistsd4.cfm.

[24] "NIST Biometric Image Software," http://www.nist.gov/itl/iad/ig/nbis.cfm.

[25] L. Hong, Y. Wan, and A. Jain, "Fingerprint image enhancement: algorithm and performance evaluation," *IEEE Transactions on Pattern Analysis and Machine Intelligence*, vol. 20, no. 8, pp. 777–789, 1998.

[26] K. G. Larkin and P. A. Fletcher, "A coherent framework for fingerprint analysis: are fingerprints holograms?" *Optics Express*, vol. 15, no. 14, pp. 8667–8677, 2007.